SOURCE PARAMETERS OF THE LEFT VENTRICLE RELATED TO THE PHYSIOLOGICAL CHARACTERISTICS OF THE CARDIAC MUSCLE

R. BEYAR, AND S. SIDEMAN
Departments of Chemical and Biomedical Engineering, The Julius Silver Institute of Biomedical Engineering, Technion-Israel Institute of Technology, Haifa, 32000, Israel

ABSTRACT An attempt is made here to correlate the physiological muscle parameters with the dynamic source parameters of the left ventricle (LV), i.e. the source (isovolumic) pressure P_o and the source (internal) resistance, R_s. The internal resistance is described here as a time-dependent parameter, corresponding to the pressure drop (from the theoretical instantaneous isovolumic pressure) associated with the instantaneous ejection flow rate. The source pressure, which relates to the muscle stress and the ventricular volume, is represented by the time-varying elastance concept and a spheroidal model relating the average wall stress to LV pressure. Linear and exponential force-velocity relationships (FVR), expressed in stress-strain rate terms, are compared. Two possible characteristics of the dynamic FVR in the partially active state, based on either a parallel or a fanlike shift of the stress-strain rate curve, are studied by utilizing simple analytical models as well as a computer simulation model. Comparing the calculated results with experimental data indicates that the dynamic FVR shift occurs in a fanlike pattern in which the maximum strain rate remains constant throughout the cycle. This pattern of the FVR shift is consistent with experimental data that show that the internal resistance is linearly related to the instantaneous isovolumic pressure. The analysis also indicates that the difference between the hyperbolic and linear FVR is rather minor, and in spite of some effects on the ejection pattern and the value of R_s, the functional shape has no effect on the global LV characteristics, such as the ejection fraction and stroke volume.

INTRODUCTION

Numerous attempts at modeling the cardiovascular system have led to the development of a large number of analog and digital models of the left ventricle (LV). A group of electrically oriented analogies for the LV performance are based on a pressure source that is combined, in series, with an internal source resistance, or impedance, (Elzinga and Westerhof, 1973, 1978; Westerhof et al., 1977; Abel 1966, 1971; Fich et al., 1973; Min et al., 1976, 1978; Buonochristiani et al., 1973; Shroff et al., 1983; Hunter et al., 1983). These concepts of source parameters have evolved from the Thevenin-Norton Equivalence theorem for electrical circuits that define an open circuit voltage for the electrical source, analogous to the isovolumic pressure of the LV. The in-series resistance of the system is defined as the source resistance. While the experimental data provided by Elzinga and Westerhof (1973, 1978) and Buonochristiani et al. (1973) deal with the average values of the LV pressure and the internal resistance, Welkowitz (1977, 1981) and Min (1978), have used the instantaneous pressure and flow values to characterize the LV internal impedance rather than its resistance. Shroff et al. (1983) and Hunter et al. (1983) have suggested that the instantaneous LV internal resistance may be combined with a time-varying elastance concept representing the source pressure. Relating the source parameters to the LV physiology, they have shown that the LV internal resistance is directly proportional to the theoretical isovolumic pressure at the corresponding volume and time. Fry (1964), Pollack (1970), Hugenholtz et al. (1970), and Weber and Janicki (1977) combined the force-length-velocity relationship of the heart muscle with the geometric and structural properties of ventricular wall to predict the isovolumic ventricular pressure, i.e. the source pressure. Min et al. (1976, 1978), Welkowitz (1977), Abel (1966, 1971), and Kresh et al. (1976) indicated a mathematical correlation between the macro-scale ventricular level model and the micro-scale muscle to ventricle model, based on a linear stress—(shortening) velocity relationship of heart muscle. Note that the internal impedance rather than the internal resistance concept was employed in the studies.

The source pressure selected here relates to the isovolumic elastance function $E_o(t)$ as the determinator of the instantaneous volume-dependent but flow-independent pressure. This means that the source pressure of an eject-

Please address reprint requests to R. Beyar, M.D., D.Sc., Department of Cardiology, Johns Hopkins University Hospital, 720 Ruthland Avenue, Baltimore, MD 21205.

ing LV at a certain instant is the pressure that would have been measured immediately after a volume clamp at that instant. This definition of the pressure source is different from the classical LV source pressure, which is defined as the isovolumic pressure that corresponds to a constant volume at its end-diastolic value. To describe the source resistance we have preferred to adopt the approach of Hunter et al. (1979) of a time-varying resistance value. To quantitatively combine the muscle FVR approach with the LV internal resistance and pressure approach in a physiological sense, one needs a reasonable expression for the time-varying FVR. While data regarding the FVR at the fully active state is available in the literature (Hill, 1938; Robinson, 1965), the dynamic response of the FVR must presently be stipulated. Either hyperbolic (Fig. 1 *B*) (Beyar and Sideman, 1984*a*), or linear (Fig. 1 *A*) (Beyar and Sideman 1984*b*) FVRs can be assumed. Also, the dynamic FVR curves at the partially active states can be represented by assuming a constant ratio of the instantaneous isometric stress to the instantaneous value of the unloaded shortening velocity (or strain rate). This assumption is represented in Fig. 1 (*top*) by the partially activated FVR curves lying parallel to the fully activated FVR line. As shown in Fig. 1 (*bottom*), a different dynamic shift of the FVR during the activation cycle may be stipulated, whereby the maximum strain rate value remains constant throughout the cycle while the stress varies during the partially activated state.

The object of this study is to develop a quantitative expression for the internal resistance of the cardiac chamber as a function of time and the LV volume by combining the classical physiological and mechanical properties of the cardiac muscle with appropriate geometrical assumptions. Special scrutiny is given to the effect of the functional characteristics of the force- (or stress-) velocity relationship, either linear or hyperbolic, and to the form of the dynamic shift of this relationship in the partially active state. The LV behavior is then simulated for a variety of loading conditions by using the recently developed (spheroidal) LV model (Beyar and Sideman, 1984*a*), which relates the temporal stress, strain, and strain rate of the LV wall to the associated hemodynamic conditions. The analysis shows the interrelationships between the assumed forms of the FVR. When compared with experimental data on the time variability of the source resistance, the analysis suggests that the dynamic FVR, which changes while maintaining a constant maximum strain rate, is a better description of the dynamic FVR than the parallel shift stipulation.

GLOSSARY

a, b	constants, Eq. 15
EF	ejection fraction
$E(t)$	time varying elastance, Eq. 11
$E_o(t)$	isovolumic time varying elastance, Eq. 12
h	LV wall thickness
k	LV semimajor to semiminor axis ratio
P	LV pressure
P_o	LV isovolumic pressure

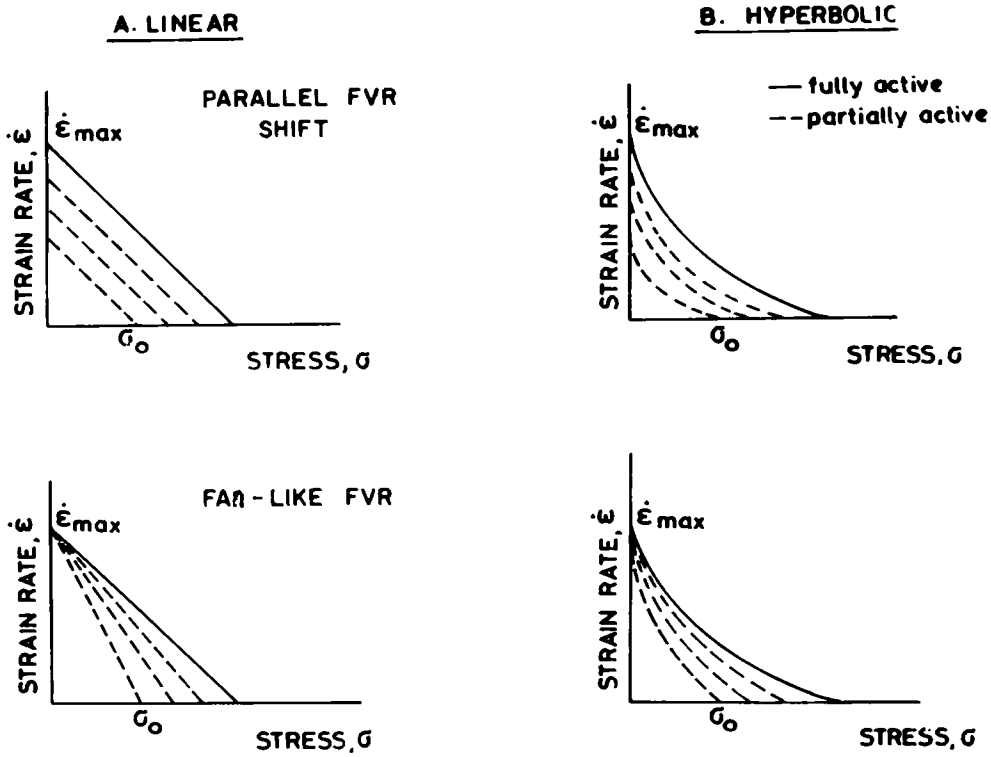

FIGURE 1 Linear (*A*) and hyperbolic (*B*) FVRs expressed in terms of strain rate and stress. Note that the dynamic shift during the LV contraction may be assumed as a parallel shift (*top*) or a fanlike shift (*bottom*) hinging on the $\dot{\epsilon}_{max}$ value.

Q	LV outflow
R_s	LV internal resistance
r	LV semiminor axis
V_{max}	maximum shortening velocity of the fibers
V	LV volume
V_0	minimal LV volume needed for active stress development
V_{ed}, V_{es}	end diastolic and end systolic LV volumes, respectively
α	maximum value of $E_0(t)$
ϵ	strain
$\dot{\epsilon}$	strain rate
$\dot{\epsilon}_{max}$	maximum strain rate
σ	stress (circumferential)
σ_0	isovolumic stress.

ANALYTICAL EVALUATION OF THE LV SOURCE RESISTANCE

1. Linear Stress-Strain Rate (Velocity) Relationship

Consider the LV as a spheroid (Fig. 2) with an endocardial semiminor axis r, a semimajor to semiminor axis ratio $k = 2$ and a wall thickness h. The linear active stress-strain rate relationship for the cardiac muscle, proposed by Ross et al. (1966) and Robinson (1965), and shown in Fig. 1 A, is represented by

$$\dot{\epsilon} = \dot{\epsilon}_{max}\left(\frac{\sigma_0 - \sigma}{\sigma_0}\right), \tag{1}$$

where $\sigma = \sigma(t)$ is the circumferential time dependent stress at the equator, $\sigma_0 = \sigma_0(t)$ is the instantaneous (isovolumic) circumferential stress, $\dot{\epsilon} = \dot{\epsilon}(t)$ is the circumferential time-dependent endocardial strain rate (which is also equal to the meridional strain rate since the shape of the LV is assumed to remain practically unchanged during the contraction). $\dot{\epsilon}_{max}$ is the maximum strain rate, linearly related to σ_0 for the parallel shift and constant for the fanlike shift. Note that as σ_0 is a function of time (and volume), the instantaneous FVR changes accordingly. The parallel-shift form is associated with a constant $\dot{\epsilon}_{max}/\sigma_0$ ratio. The fanlike shift form shows that the FVR shifts to the left while hinging on $\dot{\epsilon}_{max}$, which remains constant as σ_0 changes throughout the cycle.

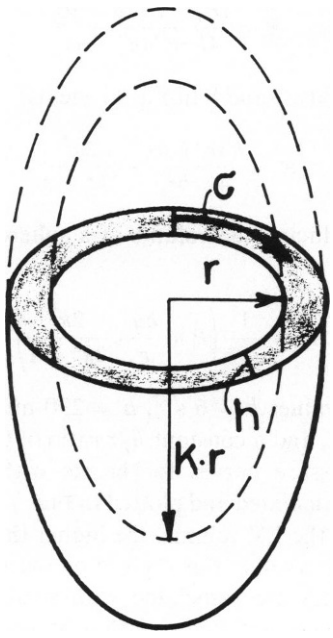

FIGURE 2 The spheroidal geometry of the LV. The semiminor axis is denoted as r, the semimajor axis is defined as kr, where k is constant. h-wall thickness. Note the circumferential stress σ.

The circumferential strain rate for the inner layers is given by

$$\dot{\epsilon} = \frac{1}{r}\frac{\mathrm{d}r}{\mathrm{d}t}. \tag{2}$$

Note that the internal radius rather than the midwall radius is used here throughout as the representative radius. (This approach, albeit approximate, avoids the need to trace the moving midpoint through the cycle while still retaining the essential features of the analysis).

The instantaneous source (internal) resistance R_s of an ejecting LV is defined here according to the studies of Hunter et al. (1979, 1983), and Shroff et al. (1983). Using the pressure drop ΔP between the theoretical isovolumic (zero flow) pressure P_0 (representing the source pressure at the corresponding clamped volume and time during the cycle) and P, the actual LV pressure, R_s is given by

$$R_s = \frac{P_0 - P}{Q} = \frac{\Delta P}{Q}, \tag{3}$$

where Q denotes the aortic flow, consistent with Hunter et al. (1979, 1983) and Shroff et al. (1983), whereby a flow pulse Q into the LV yields a pressure shift ΔP. For the assumed spheroidal LV, Q is given by

$$Q = \frac{\mathrm{d}V}{\mathrm{d}t} = 4k\pi r^2\frac{\mathrm{d}r}{\mathrm{d}t}. \tag{4}$$

Combining Eqs. 2 and 4 yields

$$Q = 4k\pi r^3\dot{\epsilon}. \tag{5}$$

Eqs. 1, 3, and 5 yield

$$R_s = \frac{(P_0 - P)\sigma_0}{4k\pi r^3\dot{\epsilon}_{max}(\sigma_0 - \sigma)}. \tag{6}$$

The LV cavity pressure P relates to the wall stress by (Gault et al., 1968)

$$\sigma = \frac{P \cdot r}{h}\left(1 - \frac{1}{2k^2}\right). \tag{7}$$

Similarly, the isovolumic (zero flow) source pressure P_0 is related to the instantaneous isovolumic stress σ_0 by

$$\sigma_0 = \frac{P_0 r}{h}\left(1 - \frac{1}{2k^2}\right). \tag{8}$$

Combining Eqs. 6, 7, and 8 yields

$$R_s = \frac{h\sigma_o}{4k\pi r^4 \dot{\epsilon}_{max}} \left(\frac{2k^2}{2k^2 - 1} \right) = \frac{h\sigma_o}{3rV\dot{\epsilon}_{max}} \left(\frac{2k^2}{2k^2 - 1} \right). \quad (9)$$

Introducing Eq. 8 into Eq. 9 yields the relationship between R_s and the isovolumic pressure P_o

$$R_s = \frac{P_o}{3\dot{\epsilon}_{max} V}. \quad (10)$$

The cavity pressure P is related to the instantaneous elastance function $E(t)$ by (Suga et al., 1973, 1976; Suga and Sagawa, 1974; Suga and Yamakoshi, 1977)

$$P = E(t) \cdot (V - V_o), \quad (11)$$

where V_o is a constant representing the LV cavity volume corresponding to a zero active stress. However, it is noted that the value of P and hence the value of $E(t)$ depend on the instantaneous flow. To avoid this dependency, the value of the isovolumic elastance $E_o(t)$, rather than $E(t)$, is used, yielding

$$P_o = E_o(t) \cdot (V - V_o). \quad (12)$$

Substituting Eq. 12 in Eq. 10 yields

$$R_s = \frac{V - V_o}{V} \cdot \frac{E_o(t)}{3\dot{\epsilon}_{max}}. \quad (13)$$

Eqs. 13 and 9 can now be related to the two forms of the dynamic FVR to yield the following conclusions: (*a*) $\dot{\epsilon}_{max}$ is constant in the fanlike hinged-type FVR form, and R_s is almost linearly proportional to $P_o = P_o(t)$, provided that the volume is constant, as is consistent with Eqs. 10 or 13. Some deviation from this relationship is caused by the term $(V - V_o)/V$, but this has only a second order effect. (*b*) $\dot{\epsilon}_{max}$ and σ_o change simultaneously in the parallel shift case. As σ_o is related to $E_o(t)$ the ratio $E_o(t)/\dot{\epsilon}_{max}$ in Eq. 13 is less variable than in the fanlike case, and R_s is less variable in this case than in the previous one.

The two dynamic FVR forms in Fig. 1 *A* converge at end-systole into a single form as $\dot{\epsilon}_{max}$ reaches its maximum value. At this point $V = V_{es}$, $E_o(t) \rightarrow \alpha$ and

$$R_s = \frac{V_{es} - V_o}{V_{es}} \frac{\alpha}{3} \left(\frac{1}{\dot{\epsilon}_{max}} \right). \quad (14)$$

For a fully activated canine heart with a maximum elastance value (Sonnenblick, 1965; Taylor et al., 1967) $\alpha = 4$ mmHg/ml, $\dot{\epsilon}_{max} = 3$ circumferences/s, $V_o = 10$ ml, $V_{es} = 25$ ml and the corresponding value of the internal resistance R_s (end-systole) = 0.26 mmHg s/ml.

Shroff et al. (1983) have characterized R_s as a function of P_o. Canine hearts, characterized by $\alpha = 4.6$ mmHg/ml and beating isovolumically at $V = 50$ to 40 ml, yield a linear relationship between R_s and P_o, with a slope of $0.2 \cdot 10^{-2}$ s/ml. The corresponding calculated slope for the same data, utilizing Eq. 10, is

$$\text{slope} = \frac{1}{3V\dot{\epsilon}_{max}} \simeq 0.2 \text{ to } 0.27 \cdot 10^{-2} \text{ s/ml},$$

which is in good agreement with the experimental value.

2. The Hyperbolic Stress-Strain Rate Relationship

Hill's (1938) classical FVR for a skeletal muscle is commonly assumed to apply to the cardiac muscle for a fully active state. Using stress instead of force and strain rate instead of velocity, Hill's equation takes the following form:

$$(\sigma + a)\,\dot{\epsilon} = b\,(\sigma_o - \sigma), \quad (15)$$

where a, b, and σ_o are characteristic values. Note that Hill's original equation relates to a fully activated skeletal muscle (with a, b, and σ_o constants, i.e., $\sigma_o = \sigma_o(t)$), whereas here we relate to the instantaneous values of σ_o (t) as activation is increasing or decreasing. $\dot{\epsilon} = \dot{\epsilon}_{max}$, at $\sigma =$ o and Eq. 15 reduces to

$$\dot{\epsilon}_{max} = \frac{b\sigma_o}{a}. \quad (16)$$

As in the case of the linear FVR, two dynamic forms of the FVR (Fig. 1 *B*) are considered here. The parallel FVR form is associated with $\dot{\epsilon}_{max}/\sigma_o =$ constant, and as $\dot{\epsilon}_{max} = \sigma_o \cdot b/a$ at $\sigma =$o, then $b/a =$ constant. The fanlike FVR corresponds to a constant $\dot{\epsilon}_{max}$. Since $\sigma_o = \sigma_o(t)$, then $a = a(t) = b\,\sigma_o/\dot{\epsilon}_{max}$ for a constant b.

Eqs. 15, 3, and 5 yield

$$R_s = \frac{(P_o - P)(\sigma + a)}{4k\pi r^3 b(\sigma_o - \sigma)}. \quad (17)$$

Substituting Eqs. 7 and 8 in Eq. 17 yields

$$R_s = \frac{h(\sigma + a)}{4k\pi b r^4} \cdot \frac{2k^2}{2k^2 - 1}. \quad (18)$$

Finally, introducing the volume of a spheroid into Eq. 18 gives

$$R_s = \frac{1}{3Vb} \left(P + \frac{ha}{r} \cdot \frac{2k^2}{2k^2 - 1} \right). \quad (19)$$

Using the values $b = 6\ s^{-1}$, $a = 230$ mmHg, $\sigma_o = 115$ mmHg, $k = 2$, and a constant h/r ratio of 0.45, a series of resistance-pressure curves for hearts with different LV volumes are calculated and plotted in Fig. 3. As seen in Fig. 3, the smaller the LV volume, the higher the resistance for a given pressure value. For a given pressure-driving force, smaller volumes are associated with smaller strain rates and smaller flows and hence with a higher internal resistance. Note that R_s increases as the value of P_o increases (Eq. 10). The nonlinear dependence of R_s on the LV volume given by Eq. 19 is shown in Fig. 4 for a pressure of

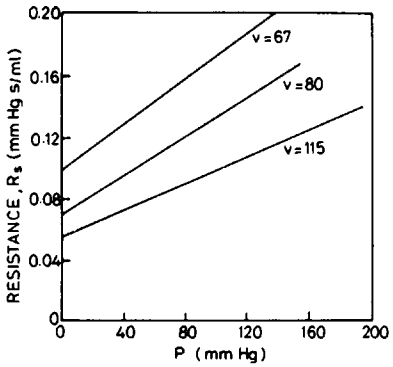

FIGURE 3 The LV source resistance as a function of the pressure P for different hearts with different LV volumes (Eq. 19).

100 mmHg. As seen, higher resistance values are encountered with smaller LV.

Combining Eqs. 11 and 19 gives

$$R_s = \frac{1}{3Vb}\left[E(t)\cdot(V - V_0) + \frac{ha}{r}\cdot\frac{2k^2}{2k^2 - 1}\right]. \quad (20)$$

Taking $V \gg V_0$ and $k^2 \gg 1$ as a very rough approximation, Eq. 20 reduces to

$$R_s \simeq \frac{1}{3b}\left[E(t) + \frac{ah}{rV}\right]. \quad (21)$$

It is suggested that for different preloads, i.e. different initial volumes, the value of a changes so that $\dot{\epsilon}_{max}$ remains constant (Noordergraaf, 1978). Utilizing Eq. 8 in Eq. 16 yields

$$a = \frac{b\sigma_0}{\dot{\epsilon}_{max}} = \frac{bP_0r}{h\dot{\epsilon}_{max}}\left(\frac{2k^2-1}{2k^2}\right). \quad (22)$$

Introducing Eq. 12 with α, the maximum elastance value, replacing $E(t)$ in Eq. 22, yields

$$a = \frac{rb\alpha(V - V_0)}{h\,\dot{\epsilon}_{max}}\cdot\left(\frac{2k^2-1}{2k^2}\right). \quad (23)$$

Combining Eqs. 21 and 23 yields

$$R_s = \frac{V - V_0}{3V}\cdot\left(\frac{E(t)}{b} + \frac{\alpha}{\dot{\epsilon}_{max}}\right). \quad (24)$$

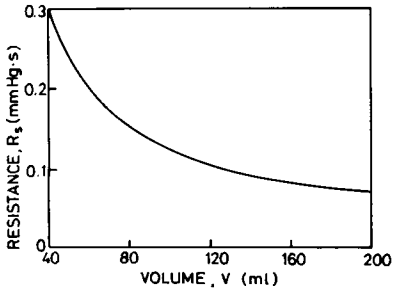

FIGURE 4 The LV source resistance as a function of the LV volume at constant pressure (Eq. 19).

Note that when $E(t) \neq \alpha$, i.e. when the muscle is not fully activated, the value of $\dot{\epsilon}_{max}$ does not reach its maximum value. This is where the difference between the two types of the dynamic FVR is most pronounced. In the case of a parallel FVR shift for the partially activated muscle, both $E(t)$ and $\dot{\epsilon}_{max}$ increase, thus inversely affecting the left and right terms in the parenthesis on the right side of Eq. 24. In the fanlike model $\dot{\epsilon}_{max}$ = constant and R_s increases with $E(t)$. When the muscle is fully activated these two cases converge and, at end-systole, become identical. Thus, at $E(t) = \alpha$ the value of $\dot{\epsilon}_{max}$ reaches its fully activated value and Eq. 24 reduces to

$$R_s\,(\text{end-systole}) = \frac{V_{es} - V_0}{V_{es}}\cdot\frac{\alpha}{3}\left(\frac{1}{b} + \frac{1}{\dot{\epsilon}_{max}}\right). \quad (25)$$

Comparing Eqs. 14 and 25 yields that at end-systole

$$\frac{R_s\,(\text{hyperbolic})}{R_s\,(\text{linear})} = 1 + \frac{\dot{\epsilon}_{max}}{b}. \quad (26)$$

For a normal set of canine data (V_{es} = 25 ml, V_0 = 10 ml, α = 4 mmHg/ml b = 6 s^{-1}, $\dot{\epsilon}_{max}$ = 3 circumferences/s) one gets R_s (hyperbolic)/R_s (linear) $\simeq$ 0.4/0.26 = 1.5. Clearly, the end-systole value of R_s based on the hyperbolic assumption is greater than R_s calculated, based on the linear assumption.

EVALUATION OF THE LV SOURCE RESISTANCE USING A COMPUTER MODEL

The interrelationships between the LV source resistance and the LV mechanics can also be evaluated independently by solving Eq. 3 directly by using the recently proposed model of the LV mechanics (Beyar and Sideman, 1984*a*), which combines the time-varying pressure-volume relationship (elastance) with the stress-velocity relationship in the LV wall. The complete cycle is described by utilizing (half) a sine function as an approximation for the time varying elastance function. A summary of the assumptions used in the simulation model is given in Table I.

The calculations begin by reading the initial conditions of the LV (end diastolic semiminor axis, aortic pressure). The isovolumic pressure P_0 is calculated using the LV volume and the time-varying elastance in steps of 0.01 s.

TABLE I
SUMMARY OF THE ASSUMPTIONS USED IN THE SIMULATION MODEL

1. The geometry is a symmetric spheroid, with an equal thickness wall.
2. A linear maximum pressure-volume relationship and half a sinusoidal time dependent elastance function apply.
3. A passive (exponential) pressure-volume curve exists.
4. Laplace law applies for the calculation of average wall stress.
5. The stress-velocity relationship relating the circumferential shortening rate to wall stress is either linear or hyperbolic.
6. A Windkessel model is used to describe the arterial system.

The aortic valve assumably opens when intraventricular pressure exceeds the aortic pressure for each step so that the intraventricular pressure, calculated from the strain rate-dependent stress, equals the aortic pressure. The outflow from the LV is then calculated from the instantaneous strain rate and the dimensions of the LV. The aortic pressure is modified in each step according to the Windkessel model. The aortic valve closes when the aortic flow is reversed. This procedure is repeated for each of the four possibilities for describing the force velocity relationship in Fig. 1.

Results of the Computer Simulation

The pressure-time, flow-time, pressure-volume, and stress volume plots for changing preloading conditions for the four cases of the FVR are shown in Fig. 5. Note that only minor differences between the four cases exist in the end systolic pressure-volume relationship. However, the dynamics of the ejection as reflected by the flow is quite different. The fanlike shifts patterns are characterized by a more rapid onset of flow at the beginning of the systole than the parallel form of the FVR, while the hyperbolic and linear cases are almost identical.

The time dependency of the internal resistance throughout the cycle for the four possible forms of the FVR is shown in Fig. 6. The corresponding isovolumic pressures P_o are also presented. R_s increases with time in the first part of the ejection in the dynamic fanlike FVR form and decreases throughout the systole in the dynamic parallel FVR case. In the fanlike shift case, R_s and P_o change in a similar parallel fashion at the beginning of ejection. The R_s values in the linear case are slightly smaller than for the hyperbolic case.

A plot of the value of R_s at the beginning of ejection vs. the corresponding value of P_o (at different afterloads) yields the results shown in Fig. 7. The figure shows how R_s linearly relates to P_o for the fanlike FVR shift, while only a slight dependency on P_o is noted for the parallel-shift case. Note that the $R_s - P_o$ slope is higher for the hyperbolic case than for the linear one.

Table II summarizes the numerically calculated values of the ejection fraction EF, end systolic volume V_{es}, and LV internal resistance R_s at the beginning and end of systole at different preload values. The latter was simulated by changing the initial semiminor axis. Minor differences in the EF are observed between the linear and the hyperbolic and parallel and fanlike cases. For the parallel-shift case, the calculated LV internal resistance based on the linear stress-velocity assumption decreases during systole to a greater extent than those based on the hyperbolic one. Increasing the preload leads to a significant increase in the

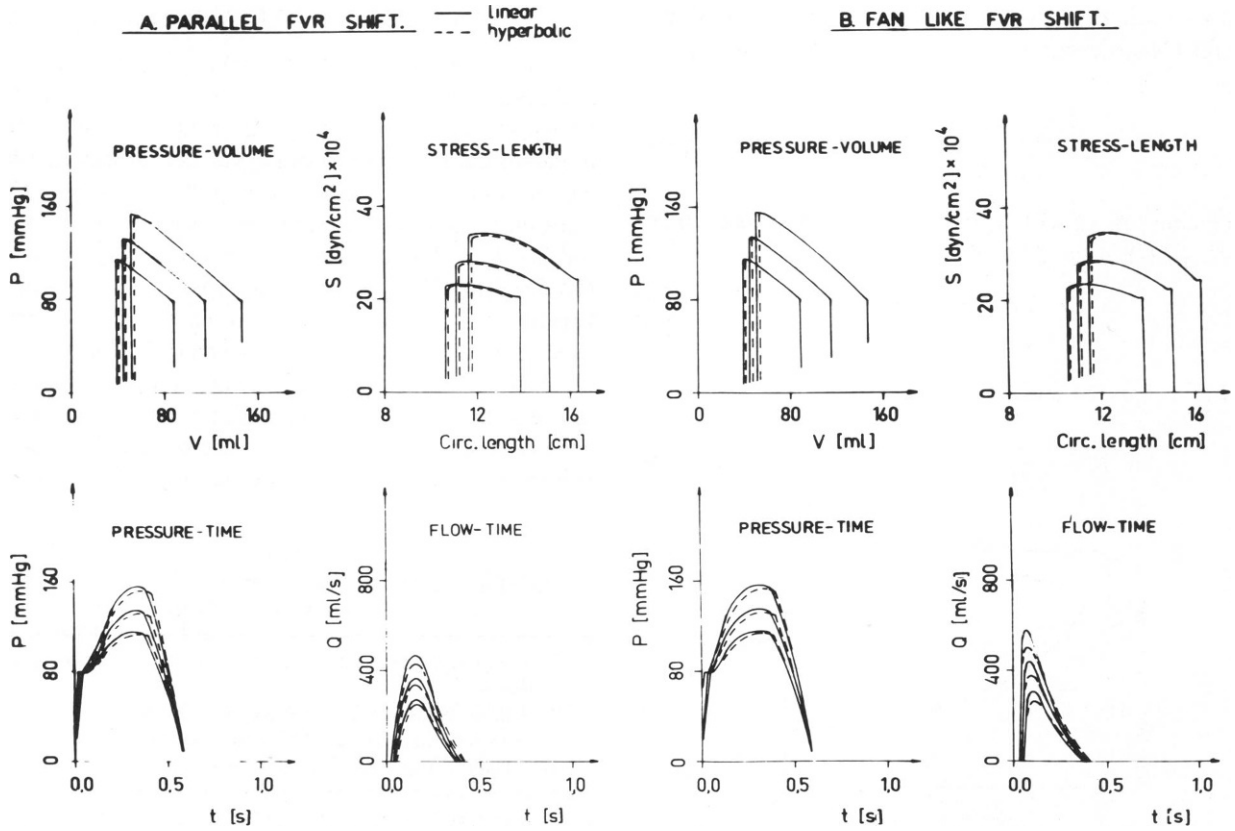

FIGURE 5 The hemodynamic function of the LV contraction for four possible cases. Parallel and fanlike FVR shifts for the linear and hyperbolic cases. Note the minor effect of the FVR on the *P-V* relationship and the greater effect on the flow curves.

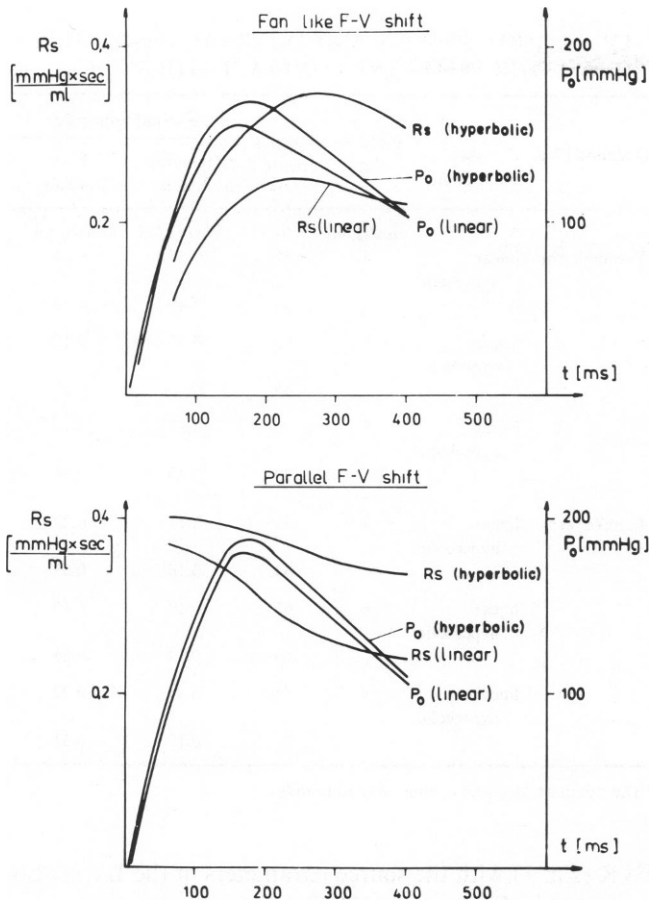

FIGURE 6 The instantaneous values of R_s and P_o for the hyperbolic and linear FVR for the fanlike and parallel FV shift. Note how R_s changes closely as P_o in the fanlike case while R_s is completely disassociated from P_o in the parallel case.

calculated R_s values based on the linear model, while R_s is only slightly affected when the hyperbolic model is used. The model shows how R_s increases from end-diastole to end-systole for the fanlike shift case.

The effects of changing the afterload are summarized in

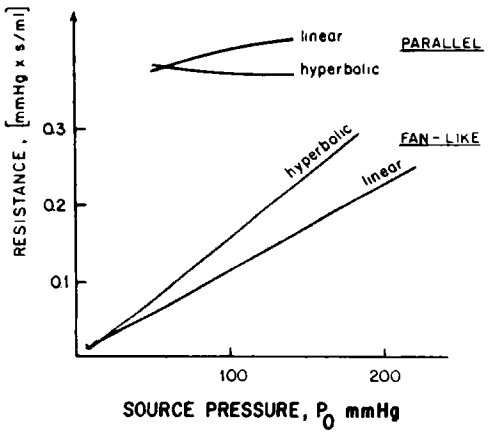

FIGURE 7 R_s at the beginning of ejection at different afterloads vs. P_o for the parallel and fanlike cases.

TABLE II
LV EJECTION INDICES AND INTERNAL RESISTANCE FOR DIFFERENT PRELOADS*

Dynamic FVR	Stress-strain rate relationship	End diastolic volume	Ejection fraction	Internal resistance	
				Beginning-systole	End-systole
		ml	*%*	*mm Hg · s/ml*	
Parallel form	linear	89	54	0.37	0.23
	hyperbolic		53	0.40	0.37
	linear	115	60	0.42	0.26
	hyperbolic		59	0.44	0.36
	linear	147	64	0.50	0.28
	hyperbolic		63	0.52	0.42
Fanlike form	linear	89	55	0.11	0.22
	hyperbolic		54	0.16	0.31
	linear	115	60	0.11	0.23
	hyperbolic		60	0.15	0.33
	linear	147	64	0.10	0.25
	hyperbolic		64	0.13	0.35

*The end diastolic aortic pressure was 80 mmHg. Contractility α = 4 mmHg/ml.

Table III. As expected, the EF decreases with an increase in the end diastolic arterial pressure and is insensitive to the form of the FVR. R_s for the linear case is only slightly affected by the afterload. The dependency of R_s on the afterload is considerable for the fanlike form, showing a linear increase with the increase in the end diastolic pressure. Again, note that the R_s values of the hyperbolic FVR are consistently higher than the values for the linear one.

The effects of changing the LV contractility are summarized in Table IV. The contractility changes are simulated here by modifying the value of the maximum elastance α which, in turn, linearly affects the value of $\dot{\epsilon}_{max}$ (Hunter et al., 1983; Shroff et al., 1983). Thus, a twofold increase in contractility is simulated by twice the original value of α and $\dot{\epsilon}_{max}$. As seen, the contractility changes are not associated with significant changes in the R_s values. The differences between the linear vs. hyperbolic and parallel vs. fanlike FVR forms as are described before.

DISCUSSION

This study attempts to demonstrate that representing the LV mechanics by time dependent source pressure and internal resistance is directly related to the classical muscle mechanics expressed by the force length-velocity relationship. The concept of the source pressure and source resistance has been referred to differently by different research groups. These include an average value for the source pressure and resistance (Elzinga and Westerhof, 1973; 1978; Westerhof and Elzinga, 1978), a frequency

TABLE III
LV EJECTION INDICES AND INTERNAL RESISTANCE FOR DIFFERENT AFTERLOADS*

Dynamic FVR	Stress-strain rate relationship	ED pressure	Ejection fraction	Internal resistance	
				Beginning-systole	End-systole
		mmHg	*%*	*mmHg s/ml*	*mmHg s/ml*
Parallel form	linear	60	59	0.38	0.23
	hyperbolic		58	0.39	0.31
	linear	90	52	0.37	0.24
	hyperbolic		51	0.41	0.35
	linear	120	46	0.37	0.27
	hyperbolic		44	0.43	0.38
Fanlike form	linear	60	59	0.10	0.23
	hyperbolic		59	0.13	0.29
	linear	90	53	0.13	0.23
	hyperbolic		51	0.18	0.32
	linear	120	46	0.17	0.25
	hyperbolic		45	0.23	0.34

*End diastolic volume = 80 ml. Contractility α = 4 mmHg/ml.

TABLE IV
LV EJECTION INDICES AND INTERNAL RESISTANCE FOR DIFFERENT CONTRACTILITIES*

Dynamic FVR	Stress-strain rate relationship	Contractility	Ejection fraction	Internal resistance	
				Beginning-systole	End-systole
		mmHg/ml	*%*	*mmHg s/ml*	*mmHg s/ml*
Parallel form	linear	4	55	0.37	0.24
	hyperbolic		53	0.40	0.33
	linear	6	65	0.37	0.19
	hyperbolic		65	0.40	0.32
	linear	8	70	0.37	0.19
	hyperbolic		70	0.40	0.31
Fanlike form	linear	4	55	0.11	0.22
	hyperbolic		54	0.16	0.31
	linear	6	65	0.10	0.19
	hyperbolic		65	0.14	0.31
	linear	8	71	0.8	0.22
	hyperbolic		71	0.12	0.31

*The end diastolic aortic pressure was 80 mmHg.

domain approach (Welkowitz 1977, 1981; Min et al., 1976, 1978; Abel 1966, 1971), and a time-dependent representation for the source pressure and internal resistance. Here, we use the time varying internal resistance approach (Hunter et al., 1979, 1983; Shroff et al., 1983) and a source pressure that seems to be directly related to the muscle FVR and the time varying isovolumic elastance, and thus has a physiologic meaning. The study proceeds by two stages. The first stage involves the development of analytical expressions for the above relation. The second stage uses a computer simulation model of the LV.

An attempt to relate the fiber FVR to the LV source parameters was reported by Min et al. (1978), who related R_s to the ventricular parameters by

$$R_s = \gamma(\epsilon)\frac{\theta}{B(t)}\frac{1}{r^2}, \tag{28}$$

where $\gamma(\epsilon)$ is a function representing the strain-dependent relation between the isovolumic force and the maximum shortening velocity; θ is a (constant) central angle for a circumferential muscle segment and $B(t)$ is related to the long axis of the ventricle. The inverse relationship between R_s and the LV dimensions in Eq. 28 is consistent with our Eq. 13. Also, changes in contractility do not affect R_s since contractility affects the maximum shortening velocity and the isovolumic force for each segment length in a similar way. A mathematical analysis relating the linear fibers FVR (Eq. 1) with the source parameters of the LV is also presented by Welkowitz (1983).

R_s AND THE DYNAMIC FVR SHIFT

The source resistance is related here to the pressure difference between P, the actual measured LV pressure, and $P_o(t)$, the theoretical isovolumic pressure at the instantaneous clamped volume value. In that sense the source parameters P_o and R_s are time-dependent, and both are related to well-established cardiac physiology. P_o is derived from the time varying elastance concept for isovolumic contractions (ignoring the effect of muscle strain rate on its stress), while R_s is derived from the FVR of the muscle.

The parametric description of R_s is closely related to the dynamic properties of the FVR. Linear and hyperbolic form of the FVR are compared here. Each of these two cases can be described by two different dynamic forms of the FVR shift with time. The parallel shift corresponds to the situation in which the partially active muscle operates with a constant $\dot{\epsilon}_{max}/\sigma_o$ ratio, while σ_o changes with the activation and the LV volume and $\dot{\epsilon}_{max}$ changes proportionally. This implies that the unloaded shortening velocity $\dot{\epsilon}_{max}$ of a muscle at a partially active state will be less than the velocity in the fully activated state. Conversely, $\dot{\epsilon}_{max}$ is kept constant in the fanlike model throughout the cycle and the unloaded shortening velocity does not depend on the degree of activation.

Inspection of the analytical and computerized numerical

results leads to a definite conclusion regarding the dynamics of the FVR. Both the analytical expression (Eq. 10) and the computer model results (Figs. 6–7) imply that R_s is proportional to P_o. The same proportionality was also found by Shroff et al. (1983) and by other investigators (Vaartjes et al., 1982). On the other hand, the parallel form of the dynamic FVR shows that R_s decreases throughout the cycle (Fig. 7, and Tables II–IV) due to the increasing value of $\dot{\epsilon}_{max}$ during the activation state (Eq. 24).

It is thus reasonable at this stage to accept the fanlike FVR form as the more appropriate description of the dynamic properties of the muscle during the activation cycle. Such a conclusion is consistent with well established experimental data that the unloaded shortening velocity for $\dot{\epsilon}_{max}$ reach the maximum value shortly after the onset of activation, (Sonnenblick, 1965; Daniels et al., 1984).

Hyperbolic vs. Linear FVR

Addressing the issues of the hyperbolic vs. the linear FVR, does not at this stage lead to experimentally confirmed conclusions. However, some of the reported experimental data may provide insight and lead to the correct formulation.

As seen here in Figs. 6–7, Eq. 26, and Tables II–IV, the value of R_s for the hyperbolic case is consistently higher than R_s in the linear case. This result is attributed to the smaller (negative) slopes of the hyperbolic FVR curves at the higher region of stresses studied (Fig. 1 *B*). A smaller (negative) slope implies that a lower strain rate is needed to achieve a given stress reduction that leads to a decreased flow for a given pressure drop ΔP. This, in turn, results in higher values of R_s for the hyperbolic case. A study of R_s as a function of the flow pulse Q (Hunter et al., 1979, 1983) may help determine the correct type of the FVR in the intact heart. Independence of R_s and Q will direct us to the linear model, whereas a decrease in R_s with Q will point at a hyperbolic FVR.

Effect of the FVR on E_{max}

It is interesting to note whether the type of the FVR function has any effect on E_{max}. The present analysis and the structural model of the LV, which is based on the fiber's properties (Beyar and Sideman 1984*b*), shows that E_{max} is practically unaffected by the FVR. For a normally functioning heart the maximum value for $E(t)$ and end ejection almost coincide. The flow at end ejection is zero by definition, hence the fiber velocity (or strain rate) is zero too. Thus the fiber force at that instant equals its isometric value and is independent of the FVR. Note that this conclusion is based on the simplified assumptions used in the present model and "second order" effects that are not included in the model (like the effect of shortening on relaxation) may eventually modify this conclusion.

R_s and the Muscle Contractility

Independent of the mode of the dynamic FVR shift, both the hyperbolic and the linear FVRs models predict only a minor dependence of R_s on the contractility. This is explained by the fact that smaller LV volumes are obtained throughout the systole when the LV performance is improved. These results are supported by experiments that demonstrate the relative independence of R_s (the real part of the source impedance) on the cardiac contractility (Kresh et al., 1976; Shroff et al., 1983). The minor effect of contractility may be better understood when inspecting Eq. 9: as both $\dot{\epsilon}_{max}$ and σ_o increase with the contractility, their ratio remain practically constant.

R_s and the LV Volume

As seen in Eqs. 10 and 19, the internal resistance of the LV increases with the decrease of the LV volume in hearts of different body sizes at comparable pressures. This inverse relationship between the internal resistance and the volume indicates in Figs. 3 and 4 that smaller hearts (of smaller species) are associated with higher values of the internal resistance. This result is consistent with the fact that the arterial impedance is greater for smaller animals. Thus, an optimal match of the LV and arterial impedances is maintained in hearts of different sizes (or species) by the corresponding parallel increase of the arterial and the ventricular impedances with the decrease in the dimensions of the LV.

SUMMARY

The mathematical analysis presented here relates the LV internal or source resistance R_s to the physiological laws governing cardiac muscle contraction by comparing the linear and the hyperbolic FVR of the cardiac muscle, both for a parallel and fanlike form of the dynamic FVR.

The results indicate that global LV parameters such as the ejection fraction are in fact insensitive to the assumed FVR form. Comparison of the calculated values of the time dependent R_s with experimental data shows that R_s is time-dependent and linearly related to the isovolumic pressure. Thus it seems that the fanlike form of the dynamic FVR relationship (with a constant $\dot{\epsilon}_{max}$) is the more physiological description of this phenomena.

This study was supported by the Michael Kennedy-Leigh Foundation, London, and the MEP Fund, Women's Division, American Technion Society, New York. We gratefully acknowledge this support and trust.

Received for publication 1 May 1984 and in final form 27 December 1985.

REFERENCES

Abel, F. L. 1976. An analysis of the left ventricle as a pressure and flow generator in the intact systemic circulation. *IEEE (Inst. Electr. Electron. Eng.) Trans. Biomed. Eng.* 13:182–188.

Abel, F. L. 1971. Fourier analysis of the left ventricular performance: evaluation of impedance matching. *Circ. Res.* 28:119–135.

Beyar, R., and S. Sideman. 1984*a*. A model for left ventricular contraction combining the force length velocity relationship with the time varying elastance theory. *Biophys. J.* 45:1167–1177.

Beyar, R., and S. Sideman. 1984*b*. Computer studies of left ventricular performance based on its fiber structure sarcomere dynamics and transmural electrical activation propagation. *Circ. Res.* 55:358–375.

Buonochristiani, J. F., A. J. Liedtke, R. M. Strong, and C. W. Urschell. 1973. Parameter estimation of left ventricular model during ejection. *IEEE (Inst. Electr. Electron. Eng.) Trans. Biomed. Eng.* 20:110–114.

Daniels, M., M. I. U. Noble, H. E. D. J. ier Keurs, and B.Wohlfart. 1984. Velocity of sarcomere shortening in rat cardiac muscle relation to force, sarcomere length, calcium and time. *J. Physiol. (Lond.).* 355:367–381.

Elzinga, G., and N. Westerhof. 1973. Pressure and flow generated by the left ventricle against different impedances. *Circ. Res.* 32:178–186.

Elzinga, G., and N. Westerhof. 1978. The effect of an increase in inotropic state and end diastolic volume on the pumping ability of the feline left heart. *Circ. Res.* 42:620–628.

Fich, S., W. Welkowitz, and S. Shastri. 1973. An equivalent pressure source for the heart. *Int. J. Eng. Sci.* 11:601–611.

Fry, O. L., D. M. Griggs, and J. C. Greenfield. 1964. Myocardial mechanics: tension-velocity-length relations of heart muscle. *Circ. Res.* 14:73–86.

Gault, J. H., J., Jr. Ross, and E. Braunwald. 1968. Contractile state of the left ventricle in man. Instantaneous tension velocity length relations in patients with and without diseases of the myocardium. *Circ. Res.* 22:451–459.

Hill, A. V. 1938. The heat of shortening and dynamic constants of muscle. *Proc. R. Soc. Lond. B. Biol. Sci.* 126–136.

Hugenholtz, P. G., R. C. Ellison, C. W. Urschel, I Mirsky, and E. H. Sonnenblick. 1970. Myocardial force velocity relationships in clinical heart disease. *Circulation.* 6:191–202.

Hunter, W. C., J. S. Janicki, K. T. Weber, and A. Noordegraaf. 1979. Flow pulse response: a new method for the characterization of ventricular mechanics. *Am. J. Physiol.* (Heart Circ. Physiol. 6[3]):H282–H292.

Hunter, W. C., J. S. Janicki, K. T. Weber, and A. Noordegraaf. 1983. Systolic mechanical properties of the left ventricle. Effect of volume and contractile state. *Circ. Res.* 52:319–327.

Kresh, J. M., B. G. Min, W. Welkowitz, C. A. Kulikowsky, and J. B. Kostis. 1976. Source impedance and internal reactive power in the impaired left ventricle. *Proc. 29th Conf. Eng. Biol. Med.* p. 215.

Min, B. G., S. Fich, J. B. Kostis, D. Doblar, and P. T. Kuo. 1976. Sensitivity and afterload independence of zero load aortic flow. *Ann. Biomed. Eng.* 4:330–342.

Min, B. G., J. M. Kresh, S. Fich, J. B. Kostis, and W. Welkowitz. 1978. Relationships between computed zero load aortic flow and cardiac muscle mechanics. *J. Biomech.* 80:227–235.

Noordergraaf, A. 1978. Circulatory System Dynamics. Academic Press Inc., New York. p. 213.

Polack, G. E. 1970. Maximum velocity: an index of contractility in cardiac muscle, a critical evaluation. *Circ. Res.* 26:111–127.

Robinson, L. A. 1965. Quantitative analysis of the control of cardiac output in the isolated left ventricle. *Circ. Res.* 17:207–221.

Ross, J., J. W. Covell, E. H. Sonnenblick, and E. Braunwald. 1966. Contractile state of the heart characterized by force velocity relations in variably afterloaded and isovolumic beats. *Circ. Res.* 18:129–163.

Shroff, S. G., J. S. Janicki, and K. T. Weber. 1983. Left ventricular systolic dynamics in terms of its chamber mechanical properties. *Am. J. Physiol.* 245 (Heart Circ. Physiol. 14):H110–H124.

Sonnenblick, E. H. 1965. Determinants of active state in heart muscle: force, velocity, instantaneous muscle length, time. *Med. Proc.* 24:1369–1409.

Sonnenblick, E. H. 1965. Instantaneous force-velocity length determinants in the contraction of heart muscle. *Circ. Res.* 6:441–451.

Suga, H., K. Sagawa, and A. Shoukas. 1973. Load independence of the instantaneous pressure volume ration of the canine left ventricle and effects of epinephrine and heart rate on the ratio. *Circ. Res.* 32:314–322.

Suga, H., and K. Sagawa. 1974. Instantaneous pressure volume relationships and their ratio in the exercised supported canine left ventricle. *Circ. Res.* 36:117–126.

Suga, H., K. Sagawa, and D. P. Koustwick. 1976. Controls of ventricular contractility assessed by pressure-volume ratio, E_{max}. *Cardiovasc. Res.* 10:582–592.

Suga, H., and D. Yamakoshi. 1977. Effects of stroke volume and velocity of ejection and end systolic pressure of canine left ventricle. *Circ. Res.* 40:445–450.

Taylor, R. R., J. Ross Jr., J. W. Covell, and E. H. Sonnenblick. 1967. A quantitative analysis of left ventricular myocardial function in intact sedated dog. *Circ. Res.* 21:99–115.

Vaartjes, S. R., J. A. Van Alste, and H. B. K. Boom. 1982. Active resistance during LV contraction (abstract). *Proc. 35th ACEMB.* 24:142.

Weber, K. T., and J. S. Janicki. 1977. Instantaneous force velocity length relations: Experimental findings and clinical correlations. *Am. J. Cardiol.* 40:740–747.

Welkowitz, W. 1977. Engineering Hemodynamics: Application to Cardiac Assist Devices. Lexington Books, Lexington, MA.

Welkowitz, W. 1981. Indices of cardiac status. *IEEE (Inst. Electr. Electron. Eng.) Trans. Biomed. Eng.* 28:553–567.

Welkowitz, W. 1983. Cardiac control mechanisms in adaptation to the left ventricular assist device. *Adv. Cardiovasc. Physiol. (Karger, Basel).* 5 (IV):102–117.

Westerhof, N., G. Elzinga, P. Sipkema, and G. C. Van der Broek. 1977. Quantitative analysis of the arterial system by means of pressure flow relationship. In Cardiovascular Flow Dynamics and Measurements. N. H. C. Hwang and N. A. Normann, editors. University Park Press, Baltimore, MD.

Westerhof, N., and G. Elzinga. 1978. The apparent source resistance of the heart muscle. *Ann. Biomed. Eng.* 6:16–32.